Frontiers of Information Technology & Electronic Engineering
www.jzus.zju.edu.cn; engineering.cae.cn; www.springerlink.com
ISSN 2095-9184 (print); ISSN 2095-9230 (online)
E-mail: jzus@zju.edu.cn

Optimal signal design strategy with improper Gaussian signaling in the Z-interference channel*

Dan LI, Shan WANG†‡, Fang-lin GU

(*College of Electronic Science and Engineering, National University of Defence Technology, Changsha 410007, China*)

†E-mail: chinafir@nudt.edu.cn

Received Jan. 10, 2017; Revision accepted Apr. 2, 2017; Crosschecked Nov. 25, 2017

Abstract: We propose a thoroughly optimal signal design strategy to achieve the Pareto boundary (boundary of the achievable rate region) with improper Gaussian signaling (IGS) on the Z-interference channel (Z-IC) under the assumption that the interference is treated as additive Gaussian noise. Specifically, we show that the Pareto boundary has two different schemes determined by the two paths manifesting the characteristic of improperly transmitted signals. In each scheme, we derive several concise closed-form expressions to calculate each user's optimally transmitted power, covariance, and pseudo-covariance of improperly transmitted signals. The effectiveness of the proposed optimal signal design strategy is supported by simulations, and the results clearly show the superiority of IGS. The proposed optimal signal design strategy also provides a simple way to achieve the required rate region, with which we also derive a closed-form solution to quickly find the circularity coefficient that maximizes the sum rate. Finally, we provide an in-depth discussion of the structure of the Pareto boundary, characterized by the channel coefficient, the degree of impropriety measured by the covariance, and the pseudo-covariance of signals transmitted by two users.

Key words: Z-interference channel; Improper Gaussian signaling; Sum-rate; Pareto boundary; Covariance; Pseudo-covariance

https://doi.org/10.1631/FITEE.1700030 **CLC number:** TN92

1 Introduction

It is universally known that proper Gaussian signals are entropy-maximizing (Neeser and Massey, 1993), and consequently they have been widely used in analyzing the capacity of channels with different characteristics, such as the Gaussian multiple-input multiple-output (MIMO) point-to-point channel (P2P) (Telatar, 1999) and the Gaussian MIMO broadcast channel (BC). Proper conventional signals with independent and equal variance on the real and imaginary components seem very convenient, but this does not necessarily hold in practice, especially when the system is widely linear (Hellings *et al.*, 2013). Recently, improper Gaussian signals, which are also known as asymmetric complex signals, have attracted increasing research interest because they can provide larger degrees of freedom and outperform proper Gaussian signals in different interference channels (ICs) (Cadambe *et al.*, 2010). The IC is a fundamental model where each user intends to send messages to its corresponding receiver while causing interference to other receivers. Particularly, in the upcoming 5G cellular system, diverse nodes, such as small, micro, pico, and femto cells, are expected to be connected in different proximities. Nevertheless, the cell association that forms these dense 5G networks will cause high co-channel interference, which presents a sophisticated challenge to the management (Agiwal *et al.*, 2016). Thus, an attractive re-

‡ Corresponding author

* Project supported by the National Natural Science Foundation of China (Nos. 61601477 and 61601482)

ORCID: Shan WANG, http://orcid.org/0000-0002-2435-3260

©Zhejiang University and Springer-Verlag GmbH Germany 2017

search topic is the achievable rate region description of an IC with improper Gaussian signals. Despite there have been extensive studies on the capacity of the K-user MIMO IC, work on the transmission of improper Gaussian signals to handle interference more effectively is still proceeding.

Numerous studies regarding the elimination of interference caused by improper Gaussian signaling (IGS) have been implemented. The advantages of IGS for interference management have been extensively investigated in the three-user IC model (Cadambe *et al.*, 2010), showing that each user employing IGS can obtain 1.2 degrees of freedom (DoF, also referred to as capacity pre-log, multiplexing gain, and effective bandwidth), which measures the number of independent signaling dimensions that are accessible in the network and approximates network capacity. The DoF with a user employing proper Gaussian signaling (PGS) is limited to less than one (Host-Madsen and Nosratinia, 2005) and the superiority of IGS is due to its ability to align interference, that is, to control the interference signal (Cadambe and Jafar, 2008). The superiority of IGS is due not only to the improvement in DoF, but also to an improvement of the achievable rate region in interference-limited channels. For instance, by separating the real and imaginary components of the channel coefficients, Ho and Jorswieck (2012) derived the achievable rate region for the two-user simple input, simple output (SISO)-IC with IGS, leading to a larger result than PGS with the same region. Furthermore, to achieve the rate boundary, a suboptimal scheme was proposed to derive the improperly transmitted parameters, i.e., covariance and pseudo-covariance of signals (Zeng *et al.*, 2013a). The same researchers extended the method to address a more complicated K-user multiple-input single-output (MISO)-IC, and obtained some interesting results (Zeng *et al.*, 2013b). IGS is also used to reduce the symbol error rate in the IC (Lagen *et al.*, 2016) and acts as an optimal approach along with the PGS applied in the MIMO-IC (Kurniawan and Sun, 2015). Except for interference mitigation in the IC, the application of IGS can create benefits in some other multiuser scenarios, such as relay-assisted communications and the BC with linear precoding (Kim *et al.*, 2012; Hellings *et al.*, 2013).

A particular IC case is Z-IC (Costa, 1985), where only one of the two receivers is disturbed by the transmitting signal related to the other receiver. As depicted in Fig. 1, it can approximate several real-world wireless communication scenarios, for example, in cellular networks where one user is located at the border of the cell and the other is located near the cell center of the neighboring cell and therefore not affected by the interference of the base station. In addition, there are many instances in city environments, such as large buildings and thick walls, which may keep one of the receivers out of the interference, while the other one is exposed, which is another Z-IC case.

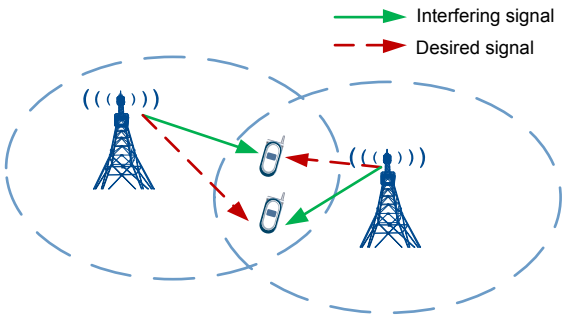

Fig. 1 Example of cell-edge users

There are several notable studies on Z-IC. The capacity region of Z-IC, which is achievable by a nonlinear processing at the receiver, is known only in strong and very strong interference regimes (Sato, 1981; Costa, 1985). Nevertheless, from a practical standpoint, adopting linear (or widely linear) processing while treating the interference as additive white Gaussian noise (AWGN) (Motahari and Khandani, 2009) brings more convenience and less complexity. Under this assumption, an optimal transmission strategy was proposed to achieve the maximum sum-rate in a SISO Z-IC (Kurniawan and Sun, 2015), which consists of five possible solutions depending on the channel characteristics, including both PGS and IGS. Furthermore, a sum-rate maximizing strategy is derived in closed form by considering the real composite model, where complex signals are denoted as real signals with double dimension. Although some limitation is involved in this kind of model, it is quite necessary to develop a more intelligent model to obtain more insightful views. Recently, a similar strategy was proposed to characterize the rate region of Z-IC by employing an augmented complex model (Lameiro *et al.*, 2017), which works with both the signal and its complex conjugate. The main

factor involved in the strategy is the circularity coefficient, which indicates the degree of impropriety. Despite some remarkable efforts of these researchers, the complexity of deriving an optimal strategy to characterize the rate region of Z-IC is still hardly affordable, and hence a more insightful and intuitive derivation of both the optimal signal design strategy and the analysis of the sum-rate is necessary and meaningful. In this study, we focus on gaining more insight into the use of IGS in Z-IC. To this end, we propose a thoroughly optimal signal design strategy to achieve the Pareto boundary, which not only proves the superiority of the use of IGS versus PGS, but also provides a quite easy way to find the optimal improperly transmitted parameters, i.e., covariance and pseudo-covariance, to fit the specific range requirement of the rate in practical applications. Furthermore, we analyze the sum-rate region on the basis of the analysis of the Pareto boundary, whereby little calculation is needed to find the variable pair that maximizes the sum-rate, which brings an intuitive view of the design of the covariance and pseudo-covariance of the signals. Nevertheless, the obtained variable pair that maximizes the sum-rate is not always optimal, and it occurs when the rate of one of the users is too low to fit the requirement in practice. To deal with this situation, an active solution is given to reduce the search space that is required to find the optimal parameters.

2 System model for Z-IC

Consider a two-user Z-IC with no symbol extensions, where each user S_r with a single antenna is intended to send a message to the corresponding receiver D_r. The process of signal transmission can be expressed as

$$y_1 = h_{11}x_1 + h_{12}x_2 + n_1, \tag{1}$$

$$y_2 = h_{22}x_2 + n_2, \tag{2}$$

where y_r and x_r are the received signal and transmitted signal at sender S_r and receiver D_r, respectively, with x_r assumed to be the improper/proper Gaussian signal. Additionally, n_r is AWGN with variance; the coefficient of channel between S_r and D_r is depicted as $h_{rk} = |h_{rk}|\,\mathrm{e}^{\mathrm{j}\phi_{rk}}$, $r, k = 1, 2$ (Fig. 2).

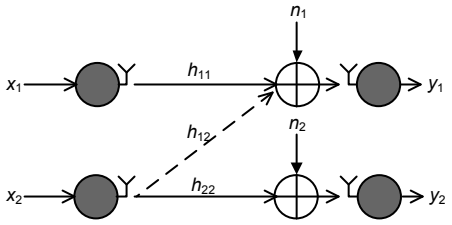

Fig. 2 The Z-IC model

2.1 Preliminary: improper random variables

The covariance of a zero-mean IRV z is described as $C_z = E[|z|^2]$. Analogously, we define the pseudo-covariance as $\tilde{C}_z = E[z^2]$. Then variable z is called proper if and only if $\tilde{C}_z = 0$; otherwise, it is called improper. Particularly, Lameiro (2017) illustrated that C_z and $\tilde{C}_z$ are a fixed pair of variance only if the condition $0 \le |\tilde{C}_z| \le C_z$ holds. So, the pseudo-covariance of z can be described as $\tilde{C}_z = |\tilde{C}_z|\mathrm{e}^{\mathrm{j}\theta}$.

2.2 Description of capacity with improper signaling

According to the definition of information entropy and channel capacity, with the assumption that interference is treated as AWGN, the achievable rate of each user can be viewed as the mutual information of the transmitted signal and received signal, which can be formulated as (Zeng *et al.*, 2013a)

$$\begin{aligned} R_i &= I(x_i; y_i) = h(y_i) - h(y_i\,|x_i\,) = h(y_i) - h(w_i) \\ &= \underbrace{\log_2 \frac{|C_{y_i}|}{|C_{w_i}|}}_{R_{\text{proper}}} + \frac{1}{2}\log_2 \frac{1 - C_{y_i}^{-2}\left|\tilde{C}_{y_i}\right|^2}{1 - C_{w_i}^{-2}\left|\tilde{C}_{w_i}\right|^2}, \end{aligned} \tag{3}$$

where C_{y_i} and $\tilde{C}_{y_i}$ are the covariance and pseudo-covariance of the received signals, respectively. They are formulated as

$$\begin{cases} C_{y_1} = C_{x_1}|h_{11}|^2 + C_{x_2}|h_{12}|^2 + \sigma^2, \\ C_{y_2} = C_{x_2}|h_{22}|^2 + \sigma^2, \\ \tilde{C}_{y_1} = \tilde{C}_{x_1}|h_{11}|^2 + \tilde{C}_{x_2}|h_{12}|^2, \\ \tilde{C}_{y_2} = \tilde{C}_{x_2}|h_{22}|^2. \end{cases} \tag{4}$$

On the other hand, C_{w_i} and $\tilde{C}_{w_i}$, with w_i defined as the term of the interference plus noise, are the covariance and pseudo-covariance of w_i, respectively, which can be obtained as

$$\begin{cases} C_{w_1} = C_{x_2}|h_{12}|^2 + \sigma^2,\ C_{w_2} = \sigma^2, \\ \tilde{C}_{w_1} = \tilde{C}_{x_2}|h_{12}|^2,\ \tilde{C}_{w_2} = 0. \end{cases} \tag{5}$$

Then, the achievable rate region for Z-IC can be defined to be the union of all achievable rate-pairs for both channels, i.e.,

$$R = \bigcup_{0\le\left|\tilde{C}_{x_i}\right|\le C_{x_i}\le P_i} (R_1(C_{x_1},\tilde{C}_{x_1},C_{x_2},\tilde{C}_{x_2}), R_2(C_{x_2},\tilde{C}_{x_2})), \tag{6}$$

where P_i is the power budget of the signal transmitted at the ith channel.

3 Achievable rate region analysis and superiority with IGS at Z-IC

Suppose a rate-pair (R_1, R_2), which is the so-called Pareto boundary when a rate-pair (R_1, R_2') or (R_1', R_2) does not exist with $R_1' > R_1$, $R_2' > R_2$. In this section, we focus on comparing the achievable rate region when the signal is either improper or proper, by analyzing the optimal transmit strategy to achieve the Pareto boundary in both situations. Furthermore, in our model, this boundary can be characterized by the derivation of optimal transmission parameters, i.e., C_{x_i} and $\tilde{C}_{x_i}$.

First of all, substituting Eqs. (4)–(6) into Eq. (3), and after several simple manipulations, the achievable rate region for each user can be expressed as

$$R_1 = \frac{1}{2}\log_2\left[\frac{\left(C_{x_1}|h_{11}|^2 + C_{x_2}|h_{12}|^2 + \sigma^2\right)^2}{\left(C_{x_2}|h_{12}|^2+\sigma^2\right)^2\left|\tilde{C}_{x_2}h_{12}^2\right|^2} - \frac{\left|\tilde{C}_{x_2}h_{12}^2\right|^2\left|1+\dfrac{\tilde{C}_{x_1}h_{11}^2}{\tilde{C}_{x_2}h_{12}^2}\right|^2}{\left(C_{x_2}|h_{12}|^2+\sigma^2\right)^2 - \left|\tilde{C}_{x_2}h_{12}^2\right|^2}\right], \tag{7}$$

$$R_2 = \frac{1}{2}\log_2\left[\left(\frac{C_{x_2}|h_{22}|^2}{\sigma^2}+1\right)^2 - \frac{\left|\tilde{C}_{x_2}h_{22}^2\right|^2}{\sigma^2}\right]. \tag{8}$$

3.1 Preliminary assumption of parameters

According to Fig. 2 and Eqs. (7) and (8), it is clear that user 1 has no impact on user 2, and thus the maximized transmit power of signal x_1 fills the optimal transmit scheme, which reflects $C_{x_1} = P_1$. In addition, the achievable rate of user 2 has no relevance to the phase of $\tilde{C}_{x_2}$. So, we can safely take $\arg(\tilde{C}_{x_2}) = 0$, and then have $\tilde{C}_{x_2} = |\tilde{C}_{x_2}|$. Furthermore, considering the expression of R_1, it is not difficult to find that we can achieve the maximum R_1 by minimizing $\left|1+\frac{\tilde{C}_{x_1}h_{11}^2}{\tilde{C}_{x_2}h_{12}^2}\right|^2$, which yields

$$\arg\left(\frac{\tilde{C}_{x_1}}{\tilde{C}_{x_2}}\right) = \arg(\tilde{C}_{x_1}) = \pi + \arg\left(\frac{h_{12}^2}{h_{11}^2}\right), \tag{9}$$

$$\left|\tilde{C}_{x_1}\right| = \min\left(\left|\tilde{C}_{x_2}\right|\cdot\frac{|h_{12}|^2}{|h_{11}|^2}, P_1\right). \tag{10}$$

Combining the previous analysis and the definition of the achievable rate region R in Eq. (6), we can come to a conclusion that R is now a function of two parameters, i.e., C_{x_2} and $|\tilde{C}_{x_2}|$, because the others either are valid or can be expressed by these two parameters.

To simplify, we can denote C_{x_2} and $|\tilde{C}_{x_2}|$ as x and x', respectively. We already know that the relationship between the two parameters is $0 \le x' \le x$, which is distinctly shown as the shadow in Fig. 3.

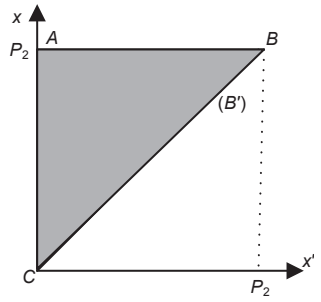

Fig. 3 Achievable domain for two parameters

3.2 Covariance optimization

When the signal is proper, we have $x' = 0$, which corresponds to vector $\boldsymbol{AC}$. From Eq. (10) we observe that the signal x_1 must be proper with $\tilde{C}_{x_1} = 0$ if signal x_2 is proper, i.e., $\tilde{C}_{x_2} = 0$. Similarly, if signal x_2 is improper, i.e., $\tilde{C}_{x_2} \ne 0$, then the signal x_1 must also be improper with $\tilde{C}_{x_1} \ne 0$.

3.3 Pseudo-covariance optimization

According to the definition of the Pareto boundary, the boundary of the rate-pair (R_1, R_2) is composed of the set of the elements where each value of R_2, corresponding to all values of R_1 varying from the minimum to the maximum, achieves the maximum.

With all the assumptions in Section 3.1, R_1 and R_2 can be rewritten as

$$R_1(x,x')=\begin{cases}\dfrac{1}{2}\log_2\dfrac{\left(P_1|h_{11}|^2+x|h_{12}|^2+\sigma^2\right)^2}{\left(x|h_{12}|^2+\sigma^2\right)^2-\left(x'|h_{12}|^2\right)^2},\\ \qquad \text{if } x'<P_1\dfrac{|h_{11}|^2}{|h_{12}|^2},\\ \dfrac{1}{2}\log_2 1+\dfrac{2P_1|h_{11}|^2}{x|h_{12}|^2+\sigma^2-x'|h_{12}|^2},\\ \qquad \text{if } x'\geq P_1\dfrac{|h_{11}|^2}{|h_{12}|^2},\end{cases}$$

$$R_2(x,x')=\frac{1}{2}\log_2\left[\left(\frac{x|h_{22}|^2}{\sigma^2}+1\right)^2-\left(\frac{x'|h_{22}|^2}{\sigma^2}\right)^2\right]. \tag{11}$$

From Eq. (11), R_1 is strictly increasing with x and strictly decreasing with x', while R_2 is strictly decreasing with x and strictly increasing with x'. Consequently, it is obvious in Fig. 3 that point A corresponds to the rate-pair $(R_{1\min}, R_{2\max})$, while point C corresponds to $(R_{1\max}, R_{2\min})$. For the deeper study, we denote the two paths from A to C as: (1) path 1 which is the vector from A to B, then to C in the condition $P_2|h_{12}|^2 \leq P_1|h_{11}|^2$ or the vector from A to B, then from $B'(P_1|h_{11}|^2/|h_{12}|^2, P_1|h_{11}|^2/|h_{12}|^2)$ to C in the condition $P_2|h_{12}|^2 > P_1|h_{11}|^2$; (2) path 2 which is the direct vector from A to C.

Theorem 1 The value of function $R_1(x,x')$ increases along both path 1 and path 2, while the value of function $R_2(x,x')$ is strictly decreasing along both path 1 and path 2.

Proof Refer to Appendix A.

Theorem 2 According to Theorem 1, we can obtain two lines, L_1 and L_2, which include all the rate-pairs with two variables that change along the two paths, respectively. Consider a rate-pair (m, n_0) on L_2, corresponding to the rate-pair (m, n_1) on L_1 (Fig. 4). Then the Pareto boundary can be denoted as the union of rate-pairs (m,n) and $n=\max(n_0,n_1)$.

Proof Refer to Appendix B.

Notice: We would like to stress that the achievable rate region when the signal is improper always contains the achievable rate region when the signal is proper. This means that proper signaling is a special case of improper signaling and exactly indicates the superiority of IGS. Particularly, taking Eq. (C2) into account when $|h_{12}|^2/|h_{22}|^2 \geq 1$ holds,

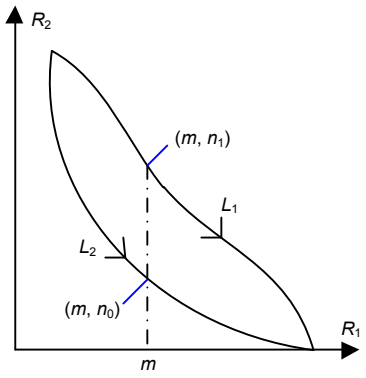

Fig. 4 Rate-pairs with variables changing along path 1 and path 2

the Pareto boundary can be achieved by changing variables along path 1, which indicates the unconditional superiority of IGS.

3.4 Optimal parameter strategy

Defining $R_1(x,x')=m$, $R_2(x,x')=n$, $R_1(0,P_2)=a_1$, $R_2(0,P_2)=a_2$, $R_1(P_2,P_2)=b_1$, $R_2(P_2,P_2)=b_2$, $R_1(0,0)=c_1$, and $R_2(0,0)=c_2$, and using Theorem 1 and Theorem 2, the optimal variable pair, (x',x), which maximizes $R_2(x',x)$ when $R_1(x',x)$ takes a valid value of m, can be characterized by the following schemes:

Power-limited region: $a_1 \leq m \leq b_1 \Leftrightarrow b_2 \leq n \leq a_2$:

Condition	Optimal variable pair (x,x')
$R_2(0,x_2) \leq R_2(x_0',x_2)$	(x_0',P_2)
$R_2(0,x_0) > R(x_0',x_0')$	$(0,x_0)$

where x_0' satisfies $R_1(x_0',P_2)=m$.

Interference-limited region: $b_1 < m \leq c_1 \Leftrightarrow c_2 \leq n < b_2$:

Condition	Optimal variable pair (x,x')
$R_2(0,x_0) \leq R_2(x_0',x_0')$	(x_0',x_0')
$R_2(0,x_0) > R(x_0',x_0')$	$(0,x_0)$

where x_0' satisfies $R_1(x_0',x_0')=m$.

Notice: We would like to indicate that when $a_1 \leq m \leq b_1$, we have

$$\lim_{P_2\to\infty}\max_{0\leq|\tilde{C}_{x_2}|\leq P_2} R_2(|\tilde{C}_{x_2}|)=\infty, \tag{12}$$

which demonstrates that R_2 is asymptotically limited by its power budget. The rate region of user 1,

$a_1 < m \leq b_1$, is called the power-limited region; when $b_1 < m \leq c_1$, we have

$$\lim_{P_2\to\infty} \max_{0\leq|\tilde{C}_{x_2}|\leq P_2} R_2(|\tilde{C}_{x_2}|) < \infty, \tag{13}$$

which demonstrates that R_2 is asymptotically limited by interference. The rate region of user 1, $b_1 < m \leq c_1$, is called the interference-limited region in Eq. (13). Note that with a fixed interference power, the lower the signal-to-noise ratio (SNR) is, the lower the achievable rate will be. In other words, when R_1 is low, and therefore R_2 is high, the interference plays a more significant role, which will be shown in detail in the next section.

In summary, this strategy provides a quick approach to find the optimal parameter with the specific requirement of rate pair (R_1, R_2), which will be discussed thoroughly in the next section.

4 Analysis and numerical results

In this section, we offer a series of discussions on the derived characterization together with some numerical results from several representative examples, to illustrate most of the features of IGS at Z-IC. The sum-rate is also analyzed and some remarkable conclusions are derived.

4.1 Sum-rate analysis

4.1.1 Sum-rate with proper signaling

As mentioned in the previous section, proper signaling corresponds to path 2. Hence, the sum-rate is characterized only by x, and can be expressed as

$$\begin{aligned} R_{\text{sum}}(x) &= R_1(0,x) + R_2(0,x) \\ &= \log_2 \frac{\left(P_1|h_{11}|^2+x|h_{12}|^2+\sigma^2\right)\left(x|h_{22}|^2+\sigma^2\right)}{\sigma^2\left(x|h_{12}|^2+\sigma^2\right)}. \end{aligned} \tag{14}$$

We thus obtain

$$\begin{aligned} \frac{\partial R_{\text{sum}}}{\partial x} = &\frac{1}{2^{R_{\text{sum}}}\sigma^2\ln 2}\cdot\frac{|h_{22}|^2}{\left(x|h_{12}|^2+\sigma^2\right)^2} \\ &\cdot\left[\left(x|h_{12}|^2+\sigma^2\right)^2+\left(1-\frac{|h_{12}|^2}{|h_{22}|^2}\right)\sigma^2P_1|h_{11}|^2\right]. \end{aligned} \tag{15}$$

Obviously, $\partial R_{\text{sum}}/\partial x > 0$ holds in the case of $|h_{12}|^2/|h_{22}|^2 \leq 1+\sigma^2/P_1|h_{11}|^2$; i.e., R_{sum} decreases as the variable changes along path 2. Thus, R_{sum} should achieve the maximum at point $R_{\text{sum}}(P_2)$. On the other hand, when

$$\frac{|h_{12}|^2}{|h_{22}|^2} \geq 1+\frac{\left(P_2|h_{12}|^2+\sigma^2\right)^2}{\left(P_1|h_{11}|^2\sigma^2\right)}, \tag{16}$$

it can be similarly derived that R_{sum} can achieve the maximum at point $R_{\text{sum}}(0)$. Finally, when

$$1+\frac{\sigma^2}{P_1|h_{11}|^2} < \frac{|h_{12}|^2}{|h_{22}|^2} < 1+\frac{\left(P_2|h_{12}|^2+\sigma^2\right)^2}{\left(P_1|h_{11}|^2\sigma^2\right)}, \tag{17}$$

R_{sum} should achieve the maximum at point $R_{\text{sum}}(0)$ or $R_{\text{sum}}(P_2)$.

In summary, the maximum sum-rate can be easily obtained with proper signaling, and we can denote the maximum value of the sum-rate in this situation as $\max(R_{\text{sum}}(P_2), R_{\text{sum}}(0))$.

4.1.2 Sum-rate with improper signaling

When IGS is employed, variation of the sum-rate results in more complex parameters. As presented in the previous section, proper signaling corresponds to path 2. Nevertheless, by several similar derivations, the conclusion is presented concisely:

Theorem 3 The distribution of the maximum sum-rate is as follows:

Case I: $|h_{12}|^2 < |h_{22}|^2$.

The point at which the maximum sum-rate is achieved is $(0, P_2)$.

Case II: $|h_{12}|^2 = |h_{22}|^2$.

The point at which the maximum sum-rate is achieved is (x_0', P_2), where $x_0' \in [0, X]$, $X = \min(P_2, P_1|h_{12}|^2/|h_{12}|^2)$.

Case III: $|h_{12}|^2 > |h_{22}|^2$.

1. $P_2|h_{12}|^2 \leq P_1|h_{11}|^2$.

The point at which the maximum sum-rate is achieved is $(0,0)$ or (P_2, P_2).

2. $P_2|h_{12}|^2 > P_1|h_{11}|^2$.

The point at which the maximum rate is achieved is among $(0,0)$, (x_0', P_2), and (P_2, P_2), where x_0' is the minimum root of $f(x') = 0$, and satisfies $P_1|h_{12}|^2/|h_{12}|^2 < x_0' \leq P_2$.

Proof Refer to Appendix C.

Notice that Theorem 3 provides a quick way to find the optimal covariance and pseudo-covariance that maximize the sum-rate; a little effort provides

some comparison. It is satisfying when the obtained variable pair fits the conditions in practice, which means that it takes few steps to obtain the optimal signal design by Theorem 3. However, the obtained variable pair is not always optimal; for example, the maximum sum-rate may be achieved at point $(0,0)$ or $(0,P_2)$, which is obviously impractical due to the low rate of user 1 or user 2. In this case, note that Theorems 1 and 2 will work and there is less computational complexity to obtain the optimal signal design, which will be discussed thoroughly in the next section.

4.2 Numerical analysis

To investigate the properties in depth, several discussions and some examples are provided as follows.

4.2.1 Optimal strategies

Optimality of proper signaling: As pointed out in Section 3, if PGS is the optimal strategy for one user, then it is also optimal for another, which means that each point on the Pareto boundary is achieved by both users employing either PGS or IGS.

Properties of the Pareto boundary: the point on the Pareto boundary where both users can employ IGS whose impropriety is up to one (which indicates that the pseudo-covariance is equal to the covariance of the transmit signal). In Fig. 3, for user 2, the vector $\boldsymbol{B}(\boldsymbol{B}')\boldsymbol{C}$ contains all the variable pairs where a maximally improper signal is transmitted. For user 1, with the analysis in Section 3, if $P_2|h_{12}|^2 \geq P_1|h_{11}|^2$, then the points at which a maximally improper signal is transmitted occur on vector $\boldsymbol{B''B}$ with B'' $(P_1|h_{12}|^2/|h_{12}|^2, P_2)$, and hence B is the only point where both users employ the maximal IGS; otherwise, such a point does not exist. In summary, both users employ the maximal IGS at the boundary point B only if $P_2|h_{12}|^2 \geq P_1|h_{11}|^2$.

To illustrate the properties mentioned above, we introduce the following simulation examples. First, we consider the channel coefficients $h_{11} = 2 - \mathrm{j}$, $h_{12} = 1.5 - 1.5\mathrm{j}$, and $h_{22} = 1 - 2\mathrm{j}$, so $|h_{11}|^2 = 5$, $|h_{12}|^2 = 4.5$, and $|h_{22}|^2 = 5$. We take the power budgets and noise variance as $P_1 = P_2 = 15$ and $\sigma^2 = 1$. The optimal covariance and pseudo-covariance of two users are shown in Fig. 5; the Pareto boundary and the sum-rate are illustrated in Fig. 6. Notice that $P_2|h_{12}|^2 < P_1|h_{11}|^2$ holds because user 1 cannot transmit maximally improper signals on the Pareto boundary. At point B, user 2 transmits the maximally improper signal, but the pseudo-covariance of user 1 is less than the covariance. Furthermore, with $|h_{12}|^2 < |h_{22}|^2$, the sum-rate is decreasing along both paths and hence achieves the maximum at point A $(0,P_2)$ (Fig. 6), which is in agreement with Theorem 3. Secondly, we consider $|h_{11}|^2 = |h_{22}|^2 = 3.25, |h_{12}|^2 = 4.5$ and $|h_{11}|^2 = 3.25, |h_{12}|^2 = |h_{22}|^2 = 4.5$. In these two cases, $P_2|h_{12}|^2 \geq P_1|h_{11}|^2$ holds, and hence both users transmit a maximally improper signal at point B. This can be observed in Figs. 7 and 9. Furthermore, since $|h_{12}|^2 \geq |h_{22}|^2$ holds, the maximum sum-rate is achieved at point B in case 1 (Fig. 8) and at any points on vector $\boldsymbol{AB}$ in case 2 (Fig. 10), which agrees with Theorem 3.

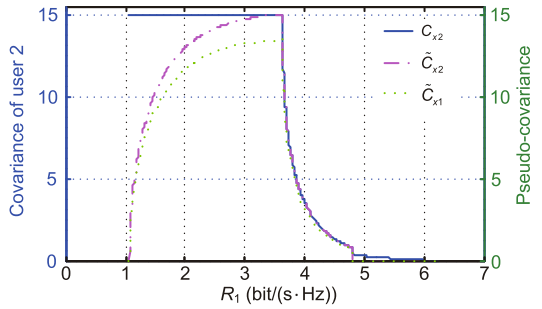

Fig. 5 Dependency of the optimal covariance and pseudo-covariance on the capacity of user 1 for $|h_{11}|^2 = 5$, $|h_{12}|^2 = 4.5$, and $|h_{22}|^2 = 5$

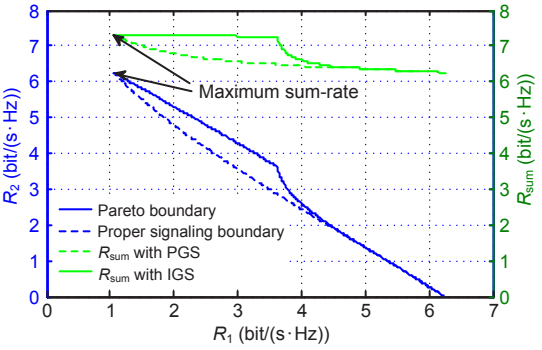

Fig. 6 Optimal rate region boundary and sum-rate with IGS and PGS for $|h_{11}|^2 = 5$, $|h_{12}|^2 = 4.5$, and $|h_{22}|^2 = 5$

4.2.2 Optimal signal design in practice

We would like to point out that the obtained variable pair that maximizes the sum-rate is not always optimal; for example, the optimal parameters occur at point $(0,0)$ or $(0,P_2)$. We introduce a quick solution to deal with this situation in the previous section, which will be investigated in Fig. 6. Consider the first case where channel coefficients are taken as $|h_{11}|^2=5$, $|h_{12}|^2=4.5$, and $|h_{22}|^2=5$. Notice that $|h_{11}|^2<|h_{12}|^2$ holds, and we can quickly obtain the variable pair $(0,P_2)$, which maximizes the sum-rate, by Theorem 3. This is absolutely not the optimal signal design, because the rate of user 1 is too small with the value of 0.77 bits/(s·Hz). If we assume that the rate of both users is not less than 3 bits/(s·Hz), then with Theorems 1 and 2, the possible region of variables of the optimal design are described as vectors $\boldsymbol{PB}$ and $\boldsymbol{BQ}$ (Fig. 11), where $P(u,P_2)$ and $Q(v,v)$ satisfy $R_1(u,P_2)=3$ bits/(s·Hz) and $R_2(v,v)=3$ bits/(s·Hz), respectively. Finally, with Theorem 3, we find that the sum-rate is decreasing along path 1; consequently, we can quickly find the optimal covariance and pseudo-covariance, i.e., (u,P_2). All of the analysis can be proved by the emulation in Figs. 5 and 6. Hence, in a specific, very complicated case, the possible region of variables of the optimal design can be easily achieved by Theorem 3 or it can be described as the definite vector, which takes less calculation or analysis to find the terminal covariance and pseudo-covariance in Z-IC.

All in all, it is obvious that the achievable rate region of improper signaling contains the entire achievable rate region of proper signaling. This can be observed in Figs. 6, 8, and 10, which show the superiority of IGS. Furthermore, the simplicity of the optimal signal design strategy proposed in Section 3 is proved adequately in this section, based on the reduction of the search space.

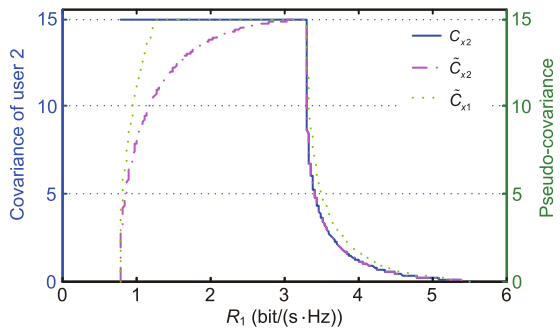

Fig. 7 Dependency of the optimal covariance and pseudo-covariance on the capacity of user 1 for $|h_{11}|^2=3.25$, $|h_{12}|^2=4.5$, and $|h_{22}|^2=3.25$

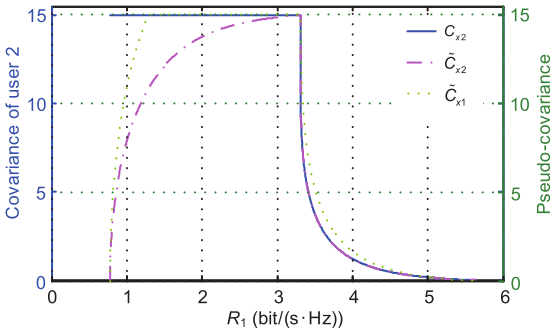

Fig. 9 Dependency of the optimal covariance and pseudo-covariance on the capacity of user 1 for $|h_{11}|^2=3.25$, $|h_{12}|^2=4.5$, and $|h_{22}|^2=3.25$

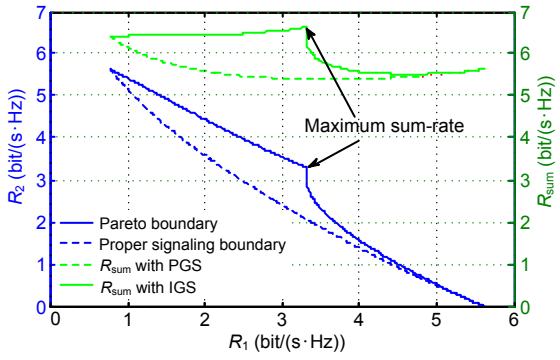

Fig. 8 Optimal rate region boundary and sum-rate with IGS and PGS for $|h_{11}|^2=3.25$, $|h_{12}|^2=4.5$, and $|h_{22}|^2=3.25$

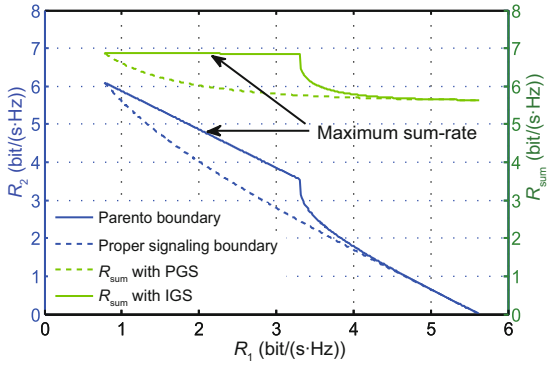

Fig. 10 Optimal rate region boundary and sum-rate with IGS and PGS for $|h_{11}|^2=3.25$, $|h_{12}|^2=4.5$, and $|h_{22}|^2=4.5$

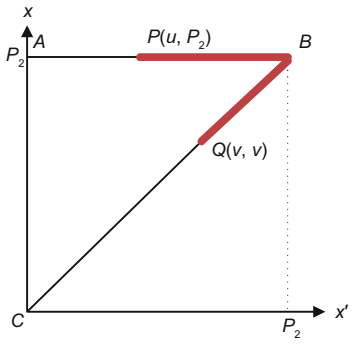

Fig. 11 The possible region of variables of the optimal design

5 Conclusions

We propose a thoroughly optimal signal design strategy to achieve the Pareto boundary with IGS in Z-IC. It is proved that the achievable rate region with IGS always contains the achievable rate region when the signal is proper, which shows the great superiority of IGS. An easy solution to achieve the required rate region is proposed through an optimal strategy, which is designed to optimize the covariance and pseudo-covariance with IGS. Furthermore, we derived a closed-form solution to achieve the maximal sum-rate, which requires less calculation to find the corresponding variable pair, i.e., covariance and pseudo-covariance.

References

Agiwal, M., Roy, A., Saxena, N., 2016. Next generation 5G wireless networks: a comprehensive survey. *IEEE Commun. Surv. Tutor.*, **18**(3):1617-1655. https://doi.org/10.1109/COMST.2016.2532458

Cadambe, V.R., Jafar, S.A., 2008. Interference alignment and degrees of freedom of the K-user interference channel. *IEEE Trans. Inform. Theor.*, **54**(8):3425-3441. https://doi.org/10.1109/TIT.2008.926344

Cadambe, V.R., Jafar, S.A., Wang, C.W., 2010. Interference alignment with asymmetric complex signaling—settling the HØst-Madsen-Nosratinia conjecture. *IEEE Trans. Inform. Theor.*, **56**(9):4552-4565. https://doi.org/10.1109/TIT.2010.2053895

Costa, M.H.M., 1985. On the Gaussian interference channel. *IEEE Trans. Inform. Theor.*, **31**(5):607-615. https://doi.org/10.1109/TIT.1985.1057085

Hellings, C., Joham, M., Utschick, W., 2013. QoS feasibility in MIMO broadcast channels with widely linear transceivers. *IEEE Signal Process. Lett.*, **20**(11):1134-1137. https://doi.org/10.1109/LSP.2013.2282186

Ho, Z.K.M., Jorswieck, E., 2012. Improper Gaussian signaling on the two-user SISO interference channel. *IEEE Trans. Wirel. Commun.*, **11**(9):3194-3203. https://doi.org/10.1109/TWC.2012.071612.111338

Host-Madsen, A., Nosratinia, A., 2005. The multiplexing gain of wireless networks. Int. Symp. on Information Theory, p.2065-2069. https://doi.org/10.1109/ISIT.2005.1523709

Kim, C., Jeong, E.R., Sung, Y.C., *et al.*, 2012. Asymmetric complex signaling for full-duplex decode-and-forward relay channels. Int. Conf. on Convergence, p.28-29. https://doi.org/10.1109/ICTC.2012.6386770

Kurniawan, E., Sun, S.M., 2015. Improper Gaussian signaling scheme for the Z-interference channel. *IEEE Trans. Wirel. Commun.*, **14**(7):3912-3923. https://doi.org/10.1109/TWC.2015.2414913

Lagen, S., Agustin, A., Vidal, J., 2016. Coexisting linear and widely linear transceivers in the MIMO interference channel. *IEEE Trans. Signal Process.*, **64**(3):652-664. https://doi.org/10.1109/TSP.2015.2489604

Lameiro, C., Santamaria, I., Schreier, P.J., 2017. Rate region boundary of the SISO Z-interference channel with improper signaling. *IEEE Trans. Commun.*, **65**(3):1022-1034. https://doi.org/10.1109/TCOMM.2016.2641948

Motahari, A.S., Khandani, A.K., 2009. Capacity bounds for the Gaussian interference channel. *IEEE Trans. Inform. Theor.*, **55**(2):620-643. https://doi.org/10.1109/TIT.2008.2009807

Neeser, F.D., Massey, J.L., 1993. Proper complex random processes with applications to information theory. *IEEE Trans. Inform. Theor.*, **39**(4):1293-1302. https://doi.org/10.1109/18.243446

Sato, H., 1981. The capacity of the Gaussian interference channel under strong interference. *IEEE Trans. Inform. Theor.*, **27**(6):786-788. https://doi.org/10.1109/TIT.1981.1056416

Telatar, E., 1999. Capacity of multi-antenna Gaussian channels. *Eur. Trans. Telecommun.*, **10**(6):585-595. https://doi.org/10.1002/ett.4460100604

Zeng, Y., Yetis, C.M., Gunawan, E., *et al.*, 2013a. Transmit optimization with improper Gaussian signaling for interference channels. *IEEE Trans. Signal Process.*, **61**(11):2899-2913. https://doi.org/10.1109/TSP.2013.2254480

Zeng, Y., Zhang, R., Gunawan, E., *et al.*, 2013b. Optimized transmission with improper Gaussian signaling in the K-user MISO interference channel. *IEEE Trans. Wirel. Commun.*, **12**(12):6303-6313. https://doi.org/10.1109/TWC.2013.103013.130439

Appendix A: Proof of Theorem 1

For path 1, from A to B, where $x = P_2$, R_1 and R_2 are functions of x', and it is obvious that $\partial R_1/\partial x' > 0$ and $\partial R_2/\partial x' < 0$; from B to C, where using Eqs. (7) and (8), it is straightforward to derive Eq. (A1).

Notice that if $P_2|h_{12}|^2 > P_1|h_{11}|^2$, we can find a point B' $(P_1|h_{11}|^2/|h_{12}|^2, P_1|h_{11}|^2/|h_{12}|^2)$, where R_1 is a constant b_1 from B to B'. On the other hand, notice that $\partial R_2/\partial x > 0$ when the argument

changes along vector $\boldsymbol{BB'}$; hence $R_1 = b_1$, and R_2 achieves the maximum at B. According to the above analysis, path 1 is from A to B, then from B' $(P_1 |h_{11}|^2 / |h_{12}|^2, P_1 |h_{11}|^2 / |h_{12}|^2)$ to C, which is denoted in Section 3. From Eq. (A1), we can observe that the argument x' changing from B' to C will lead to an increase in R_1 and a decrease in R_2. Similarly, for path 2, we can obtain that R_1 is increasing and R_2 is decreasing. Consequently, we have obtained the entire trend of these two functions along two paths, which completes the proof.

Appendix B: Proof of Theorem 2

First of all, in analysis parallel to the proof of Theorem 1, we split path 1 into two parts, i.e., $\boldsymbol{AB}$ and $\boldsymbol{BC}$. Consider the function R_1 in Eq. (11), which can be denoted as a curved surface in a three-dimensional system of coordinates. Then, the projection of a contour on the x'-x plane when R_1 takes a valid value m is the curve depicted as a dotted line in Fig. B1. The shape of the projection has some properties. The derivations are as follows: taking $R_1(x, x') = m$, then with some simplification, the mathematical expression of the projection of contour can be denoted as

$$\begin{cases} \dfrac{\left(P_1|h_{11}|^2 + x|h_{12}|^2 + \sigma^2\right)^2}{\left(x|h_{12}|^2 + \sigma^2\right)^2 - \left(x'|h_{12}|\right)^2} = 2^{2m}, \\ \qquad\qquad \text{if } x' < P_1 \dfrac{|h_{11}|^2}{|h_{12}|^2}, \\ \dfrac{2P_1|h_{11}|^2}{x|h_{12}|^2 + \sigma^2 - x'|h_{12}|^2} = 2^{2m} - 1, \\ \qquad\qquad \text{if } x' \geq P_1 \dfrac{|h_{11}|^2}{|h_{12}|^2}, \end{cases} \tag{B1}$$

and we obtain

$$\frac{\partial x}{\partial x'} = \begin{cases} \dfrac{\left(P_1|h_{11}|^2 + x|h_{12}|^2 + \sigma^2\right) x'|h_{12}|^2}{\left(x'|h_{12}|\right)^2 + P_1|h_{11}|^2\left(x|h_{12}|^2 + \sigma^2\right)}, \\ \qquad \text{if } x' < P_1 \dfrac{|h_{11}|^2}{|h_{12}|^2}, \\ \dfrac{x'}{x}, \quad \text{if } x' \geq P_1 \dfrac{|h_{11}|^2}{|h_{12}|^2}. \end{cases} \tag{B2}$$

When $x' < P_1 |h_{11}|^2 / |h_{12}|^2$, Eq. (B3) holds, and we obtain $0 < \partial x / \partial x' < 1$. Therefore, the projection of contour can be shaped as depicted in Fig. B1. Furthermore, if we substitute $R_1(x, x') = m$ into Eq. (11), we obtain Eq. (B4), and if we then substitute Eq. (15) into the expression of R_2, it can

$$\begin{aligned} \frac{\partial R_1}{\partial x} = \frac{\partial R_1}{\partial x'} &= \begin{cases} \dfrac{\sigma^2|h_{12}|^2\left(P_1|h_{11}|^2 + x|h_{12}|^2 + \sigma^2\right)}{2^{2R_2}\ln 2\left(2x\sigma^2|h_{12}|^2 + \sigma^4\right)^2}\left(x|h_{12}|^2 - P_1|h_{11}|^2\right) < 0, & \text{if } x' < P_1\dfrac{|h_{11}|^2}{|h_{12}|^2}, \\ 0, \quad \text{if } x' \geq P_1\dfrac{|h_{11}|^2}{|h_{12}|^2}, \end{cases} \\ \frac{\partial R_2}{\partial x} = \frac{\partial R_2}{\partial x'} &= \frac{|h_{22}|^2}{2^{2R_1}\sigma^2\ln 2} > 0. \end{aligned} \tag{A1}$$

$$\begin{aligned} &\left(P_1|h_{11}|^2 + x|h_{12}|^2 + \sigma^2\right) x'|h_{12}|^2 - \left[\left(x'|h_{12}|\right)^2 + P_1|h_{11}|^2\left(x|h_{12}|^2 + \sigma^2\right)\right] \\ &= \left(P_1|h_{11}|^2 - x'|h_{12}|\right)\left[x'|h_{12}| - \left(x|h_{12}|^2 + \sigma^2\right)\right] < 0. \end{aligned} \tag{B3}$$

$$x' = \begin{cases} \dfrac{1}{|h_{12}|^2}\left[\left(x|h_{12}|^2 + \sigma^2\right)^2 - 2^{-2m}\left(P_1|h_{11}|^2 + x|h_{12}|^2 + \sigma^2\right)^2\right]^{\frac{1}{2}}, & \text{if } x' < P_1\dfrac{|h_{11}|^2}{|h_{12}|^2}, \\ \dfrac{1}{|h_{12}|^2}\left[\left(x|h_{12}|^2 + \sigma^2\right) - \dfrac{2P_1|h_{11}|^2}{\left(2^{2m} - 1\right)|h_{12}|^2}\right], & \text{if } x' \geq P_1\dfrac{|h_{11}|^2}{|h_{12}|^2}. \end{cases} \tag{B4}$$

be rewritten as Eq. (B5). Finally, we obtain the derivation of R_2 as Eq. (B6).

When $x' \geq P_1 |h_{11}|^2 / |h_{12}|^2$, $\partial R_2/\partial x$ is decreasing in m. We obtain

$$\begin{aligned} &\frac{\partial R_2}{\partial x} \geq \left.\frac{\partial R_2}{\partial x}\right|_{m_{\max}=R_1(P_2,P_2)} \\ \Leftrightarrow &\frac{\partial R_2}{\partial x} \geq \frac{2|h_{22}|^2}{2^{2R_2}\sigma^2 \ln 2} > 0. \end{aligned} \tag{B7}$$

When $x' < P_1 |h_{11}|^2 / |h_{12}|^2$, we obtain

$$\begin{aligned} \frac{\partial R_2}{\partial x} \geq 0 \Leftrightarrow x \geq \frac{1}{|h_{22}|^2}\Bigg\{ &\frac{|h_{22}|^2}{|h_{12}|^2}\Big[\sigma^2\left(1-2^{-2m}\right) \\ &-2^{-2m}P_1|h_{11}|^2\Big] - \sigma^2\Bigg\}. \end{aligned} \tag{B8}$$

Notice that if we let x_0 be such that Eq. (B8) holds with equality, then it holds with inequality strictly when $x > x_0$. Consequently, when R_1 takes value of m, the variable pair where R_2 achieves the maximum must be at M or N (Fig. B1). Similarly, we can derive the conclusion of the situation when variables change along vector $\boldsymbol{AB}$, which concludes the proof.

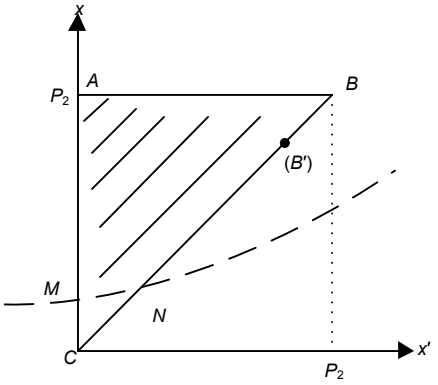

Fig. B1 Achievable domain and the projection of contour when $\boldsymbol{R_1(x, x') = m}$

Appendix C: Proof of Theorem 3

When the improperly transmitted signal is considered, we want to discuss the relevant problems under two conditions:

1. $P_2|h_{12}|^2 \leq P_1|h_{11}|^2$.

Under this condition, it is straightforward to obtain some useful results by some simple derivations. Specifically, the expression of the sum-rate when the arguments change along path 1 can be formulated as

$$\begin{aligned} R_{\text{sum}} &= R_1(x', x) + R_2(x', x) \\ &= \begin{cases} R_1(x', P_2) + R_2(x', P_2), & \text{if } a_1 \leq m \leq b_1, \\ R_1(x, x) + R_2(x, x), & \text{if } b_1 < m \leq c_1. \end{cases} \end{aligned} \tag{C1}$$

Case I: $a_1 \leq m \leq b_1 \Leftrightarrow b_2 \leq n \leq a_2$.

After a series of derivations, we can obtain Eq. (C2). Based on Eq. (C2), we can further derive

$$R_2(x) = \begin{cases} \dfrac{1}{2}\log_2\left\{\dfrac{1}{\sigma^4}\Big(x|h_{22}|^2+\sigma^2\Big)^2 - \dfrac{|h_{22}|^4}{|h_{12}|^4\sigma^4}\left[\Big(x|h_{12}|^2+\sigma^2\Big)^2 - 2^{-2m}\Big(P_1|h_{11}|^2+x|h_{12}|^2+\sigma^2\Big)^2\right]\right\}, \\ \qquad \text{if } x' < P_1\dfrac{|h_{11}|^2}{|h_{12}|^2}, \\ \dfrac{1}{2}\log_2\left\{\left(\dfrac{x|h_{22}|^2}{\sigma^2}+1\right)^2 - \dfrac{|h_{22}|^4}{|h_{12}|^4\sigma^4}\left[\Big(x|h_{12}|^2+\sigma^2\Big) - \dfrac{2P_1|h_{11}|^2}{(2^{2m}-1)}\right]^2\right\}, \\ \qquad \text{if } x' \geq P_1\dfrac{|h_{11}|^2}{|h_{12}|^2}. \end{cases} \tag{B5}$$

$$\frac{\partial R_2}{\partial x} = \begin{cases} \dfrac{2|h_{22}|^2}{2^{2R_2}\sigma^4\ln 2}\left\{x|h_{22}|^2+\sigma^2 - \dfrac{|h_{22}|^2}{|h_{12}|^2}\left[\sigma^2\left(1-2^{-2m}\right) - 2^{-2m}P_1|h_{11}|^2\right]\right\}, & \text{if } x' < P_1\dfrac{|h_{11}|^2}{|h_{12}|^2}, \\ \dfrac{2|h_{22}|^2}{2^{2R_2}\sigma^4\ln 2}\left[\sigma^2\left(1-\dfrac{|h_{22}|^2}{|h_{12}|^2}\right) + \dfrac{|h_{22}|^2}{|h_{12}|^2}\dfrac{2P_1|h_{11}|^2}{(2^{2m}-1)}\right], & \text{if } x' \geq P_1\dfrac{|h_{11}|^2}{|h_{12}|^2}. \end{cases} \tag{B6}$$

$$\begin{cases} \dfrac{\partial R_{\text{sum}}}{\partial x'^2} > 0 \Leftrightarrow \dfrac{|h_{12}|^2}{|h_{22}|^2} > 1, \\ \dfrac{\partial R_{\text{sum}}}{\partial x'^2} = 0 \Leftrightarrow \dfrac{|h_{12}|^2}{|h_{22}|^2} = 1, \\ \dfrac{\partial R_{\text{sum}}}{\partial x'^2} < 0 \Leftrightarrow \dfrac{|h_{12}|^2}{|h_{22}|^2} < 1. \end{cases} \tag{C3}$$

To be more specific, since the arguments are changing along vector $\boldsymbol{AB}$ in this case, the monotonicity of R_{sum} is determined by $|h_{12}|^2/|h_{22}|^2$. Hence, R_{sum} either is a constant or it can achieve the maximum only at point A or B, which is determined by the range of $|h_{12}|^2/|h_{22}|^2$.

Case II: $b_1 < m \le c_1 \Leftrightarrow c_2 \le n < b_2$.

$$\frac{\partial R_{\text{sum}}}{\partial x} = \frac{2|h_{12}|^2\left(P_1|h_{11}|^2 + P_2|h_{12}|^2 + \sigma^2\right)}{2^{2R_{\text{sum}}+1}\ln 2} \cdot \left[\frac{|h_{22}|^2}{|h_{12}|^2} + \sigma^2\left(1 - \frac{|h_{22}|^2}{|h_{12}|^2}\right)\frac{x|h_{12}|^2 - P_1|h_{11}|^2}{\left(2x|h_{12}|^2 + \sigma^2\right)^2}\right]. \tag{C4}$$

Let us pay attention to $|h_{12}|^2/|h_{22}|^2$. It is not hard to find that $\partial R_{\text{sum}}/\partial x > 0$ holds under the condition $|h_{12}|^2/|h_{22}|^2$. It means that R_{sum} decrease when the variables change along vector $\boldsymbol{BC}$, which is the second part of path 1. As for the case of $|h_{12}|^2/|h_{22}|^2 > 1$, we obtain that R_{sum} can achieve the maximum only at point $R_{\text{sum}}(P_2, P_2)$ or $R_{\text{sum}}(P_2, P_2)$.

2. $P_2|h_{12}|^2 > P_1|h_{11}|^2$.

Notice that if $P_2|h_{12}|^2 > P_1|h_{11}|^2$, path 1 can be denoted as from A to B, then from B' $(P_1|h_{11}|^2/|h_{12}|^2, P_1|h_{11}|^2/|h_{12}|^2)$ to A (refer to Appendix A). In this case, there exists a point M $(P_1|h_{11}|^2/|h_{12}|^2, P_2)$. Defining $R_1(P_1|h_{11}|^2/|h_{12}|^2, P_2) = b_1'$ and $R_2(P_1|h_{11}|^2/|h_{12}|^2, P_2) = b_2'$, we discuss the maximum R_{sum} in three different cases:

Case I: $a_1 \le m \le b_1' \Leftrightarrow b_2' \le n \le a_2$.

Similar to Case I in Condition 1, the monotonicity of R_{sum} with regard to the arguments x or x' is characterized by $|h_{12}|^2/|h_{22}|^2$. Hence, R_{sum} either is a constant or can achieve the maximum only at point A or B, which is determined by the value of $|h_{12}|^2/|h_{22}|^2$.

Case II: $b_1' < m \le b_1 \Leftrightarrow b_2 \le n < b_2'$.

In this situation, R_{sum} can be expressed as Eq. (C5), and the derivation can be expressed as Eq. (C6).

Let

$$f(x') = \left(x' - P_2 - \frac{\sigma^2}{|h_{12}|^2}\right)^2\left(1 - \frac{|h_{12}|^2}{P_1|h_{11}|^2}x'\right) + \sigma^2\left(2P_2 + \frac{\sigma^2}{|h_{22}|^2} + \frac{\sigma^2}{|h_{12}|^2}\right)\left(\frac{1}{|h_{22}|^2} - \frac{1}{|h_{12}|^2}\right). \tag{C7}$$

$$\frac{\partial R_{\text{sum}}}{\partial x'^2} = \frac{1}{2^{2R_{\text{sum}}+1}\ln 2} \cdot \frac{\left(P_1|h_{11}|^2 + P_2|h_{12}|^2 + \sigma^2\right)^2|h_{12}|^4|h_{22}|^4}{\left[\left(P_2|h_{12}|^2 + \sigma^2\right)^2 - (x'|h_{12}|)^2\right]^2\sigma^4} \cdot \left[\left(P_2 + \frac{\sigma^2}{|h_{22}|^2}\right)^2 - \left(P_2 + \frac{\sigma^2}{|h_{12}|^2}\right)^2\right], \tag{C2}$$

$$\begin{aligned} R_{\text{sum}} &= R_1(x', P_2) + R_2(x', P_2) \\ &= \frac{1}{2}\log_2\left\{\left[1 + \frac{2P_1|h_{11}|^2}{P_2|h_{12}|^2 + \sigma^2 - x'|h_{12}|^2}\right]\left[\left(\frac{P_2|h_{22}|^2}{\sigma^2} + 1\right)^2 - \left(\frac{x'|h_{22}|^2}{\sigma^2}\right)^2\right]\right\}. \end{aligned} \tag{C5}$$

$$\frac{\partial R_{\text{sum}}}{\partial x'^2} = \frac{P_1|h_{11}|^2|h_{12}|^2|h_{22}|^4}{2^{2R_{\text{sum}}}\sigma^4\ln 2\left(P_2|h_{12}|^2 + \sigma^2 - x'|h_{12}|^2\right)^2} \cdot \left[\left(x' - P_2 - \frac{\sigma^2}{|h_{12}|^2}\right)^2\left(1 - \frac{|h_{12}|^2}{P_1|h_{11}|^2}x'\right) + \sigma^2\left(2P_2 + \frac{\sigma^2}{|h_{22}|^2} + \frac{\sigma^2}{|h_{12}|^2}\right)\left(\frac{1}{|h_{22}|^2} - \frac{1}{|h_{12}|^2}\right)\right]. \tag{C6}$$

Then we have Eq. (C8). In this case, due to Eq. (C9), we find that $\partial R_{\text{sum}}/\partial x'^2$ decreases during the interval $[P_1\left|h_{11}\right|^2/\left|h_{12}\right|^2, (2P_1\left|h_{11}\right|^2+\left|h_{12}\right|^2P_2+\sigma^2)/(3\left|h_{12}\right|^2)]$, and increases during the interval $[(2P_1\left|h_{11}\right|^2+\left|h_{12}\right|^2P_2+\sigma^2)/(3\left|h_{12}\right|^2), P_2]$. On this basis, if $\left|h_{12}\right|^2/\left|h_{22}\right|^2 \le 1$, we have Eqs. (C10) and (C11), which indicate that R_{sum} is decreasing with x' in this case; if $P_1\left|h_{11}\right|^2/\left|h_{12}\right|^2$, we have Eq. (C12). Then, R_{sum} may achieve the maximum at $P_1|h_{11}|^2/|h_{12}|^2$, P_2, or x'_0 (which is the minimum root of $f(x')=0$, satisfying $P_1\left|h_{11}\right|^2/\left|h_{12}\right|^2 < x'_0 \le P_2$).

Case III: $b_1 < m \le c_1 \Leftrightarrow c_2 \le n < b_2$.

Similar to Case II in Condition 1, if $\left|h_{12}\right|^2/\left|h_{22}\right|^2 \le 1$, it is easy to find that R_{sum} decreases when variables change along vector $\boldsymbol{B'C}$, which is the second part of path 1. Conversely, if $\left|h_{12}\right|^2/\left|h_{22}\right|^2 > 1$, we find that the maximum can be achieved only at point B' $(P_1\left|h_{11}\right|^2/\left|h_{12}\right|^2, P_1\left|h_{11}\right|^2/\left|h_{12}\right|^2)$ or point $C\,(0,0)$. Hence, $R_{\text{sum}}(P_2,P_2) > R_{\text{sum}}(P_1\left|h_{11}\right|^2/\left|h_{12}\right|^2, P_1\left|h_{11}\right|^2/\left|h_{12}\right|^2)$ holds strictly because when variables change along vector $\boldsymbol{BB'}$, $R_1 = b_1$ and R_2 decreases.

In summary, by separating the situation into three cases, $\left|h_{12}\right|^2/\left|h_{22}\right|^2 < 1$, $\left|h_{12}\right|^2/\left|h_{22}\right|^2 = 1$, and $\left|h_{12}\right|^2/\left|h_{22}\right|^2 > 1$, we can draw a concise conclusion:

In Case I, R_{sum} achieves the maximum at $R_{\text{sum}}\,(0,P_2)$.

In Case II, R_{sum} achieves the maximum at $R_{\text{sum}}\,(x'_0,P_2)$, where $x'_0 \in [0,X]$, $X = \min(P_2, P_1\left|h_{11}\right|^2/\left|h_{12}\right|^2)$.

In Case III, when the precondition is $P_2|h_{12}|^2 \le P_1|h_{11}|^2$, R_{sum} may achieve the maximum at B (P_2,P_2) or C $(0,0)$; otherwise, when $P_2|h_{12}|^2 > P_1|h_{11}|^2$, R_{sum} may achieve the maximum at B (P_2,P_2), C $(0,0)$, or (x'_0,P_2), where x'_0 is the minimum root of $f(x')=0$, satisfying $P_1\left|h_{11}\right|^2/\left|h_{12}\right|^2 < x'_0 \le P_2$, which completes the proof.

$$\frac{\partial f(x')}{\partial x'} = \left(x'-P_2-\frac{\sigma^2}{\left|h_{12}\right|^2}\right)\left[2+\frac{\left(\left|h_{12}\right|^2P_2+\sigma^2\right)}{P_1|h_{11}|^2} - 3\frac{\left|h_{12}\right|^2}{P_1|h_{11}|^2}x'\right] \ge 0$$
$$\Leftrightarrow \frac{2P_1|h_{11}|^2+\left|h_{12}\right|^2P_2+\sigma^2}{3|h_{12}|^2} \le x' \le P_2+\frac{\sigma^2}{\left|h_{12}\right|^2}. \tag{C8}$$

$$\frac{P_1|h_{11}|^2}{\left|h_{12}\right|^2} < \frac{2P_1|h_{11}|^2+\left|h_{12}\right|^2P_2+\sigma^2}{3|h_{12}|^2} \le x' \le P_2 < P_2+\frac{\sigma^2}{\left|h_{12}\right|^2}. \tag{C9}$$

$$f\left(\frac{P_1|h_{11}|^2}{\left|h_{12}\right|^2}\right) = \frac{P_1|h_{11}|^2|h_{12}|^2|h_{22}|^4\sigma^2\left(2P_2+\frac{\sigma^2}{\left|h_{22}\right|^2}+\frac{\sigma^2}{\left|h_{12}\right|^2}\right)}{2^{2R_{\text{sum}}}\sigma^4\ln 2\left(P_2|h_{12}|^2+\sigma^2-x'|h_{12}|^2\right)^2}\left(\frac{1}{\left|h_{22}\right|^2}-\frac{1}{\left|h_{12}\right|^2}\right) \le 0. \tag{C10}$$

$$f(P_2) = \frac{\sigma^4}{\left|h_{12}\right|^4}\left(1-\frac{P_2|h_{12}|^2}{P_1|h_{11}|^2}\right)+\sigma^2\left(2P_2+\frac{\sigma^2}{\left|h_{22}\right|^2}+\frac{\sigma^2}{\left|h_{12}\right|^2}\right)\left(\frac{1}{\left|h_{22}\right|^2}-\frac{1}{\left|h_{12}\right|^2}\right) < 0. \tag{C11}$$

$$f\left(\frac{P_1|h_{11}|^2}{\left|h_{12}\right|^2}\right) = \frac{P_1|h_{11}|^2|h_{12}|^2|h_{22}|^4\sigma^2\left(2P_2+\frac{\sigma^2}{\left|h_{22}\right|^2}+\frac{\sigma^2}{\left|h_{12}\right|^2}\right)}{2^{2R_{\text{sum}}}\sigma^4\ln 2\left(P_2|h_{12}|^2+\sigma^2-x'|h_{12}|^2\right)^2}\left(\frac{1}{\left|h_{22}\right|^2}-\frac{1}{\left|h_{12}\right|^2}\right) > 0. \tag{C12}$$